Vol 17 No 5, May 2008
1674-1056/2008/17(05)/1848-06

Chinese Physics B

© 2008 Chin. Phys. Soc.
and IOP Publishing Ltd

Experimental study on parameters of dust plasma in $SiH_4/C_2H_4/Ar$ discharges*

Wu Jing(吴 静), Zhang Peng-Yun(张鹏云), Sun Ji-Zhong(孙继忠),
Zhang Jian(张 健), Ding Zhen-Feng(丁振峰), and Wang De-Zhen(王德真)†

State Key Laboratory of Materials Modification by Laser, Ion and Electron Beam, School of Physics and Optoelectronic Technology, Dalian University of Technology, Dalian 116024, *China*

(Received 21 March 2007; revised manuscript received 15 November 2007)

Measurements of dust plasma parameters were carried out in the discharges of ($SiH_4/C_2H_4/Ar$) mixtures. Dust particles were formed in the capacitively coupled radio-frequency discharge of these reactive mixtures in a cylindrical chamber. Langmuir probe was employed for diagnosing and measuring the important plasma parameters such as electron density and electron temperature. The results showed that the electron density dropped, and in contrast the electron temperature rose when the dust particles formed. The curves of the electron density and temperature versus the RF power and pressure were presented and analysed. Further, it was found that the variations of electron temperature and the size of dust void with the RF power followed the similar trends. These trends might be useful for understanding more about the characteristics of dusty voids.

Keywords: dust plasma, dust void, electron density, electron temperature, Langmuir probe
PACC: 5225Z, 5270D, 5280P

1. Introduction

In 1924, Langmuir and his colleagues[1] discovered that dust particles exist in glow discharge plasma. Since then, the formation of dust particulates in plasmas has been a well-known phenomenon. In many plasma applications, such as etching, sputtering and thin film deposition, the formation of dust particles can be readily observed. In many cases, dust particles are not welcome. For instance, in the fabrication of integrated electronic circuits（IC）, the dust particles are recognized as a main source of contamination since they could cause severe defects of the final products.[2] To prevent the formation of dust particles in plasma applications, especially in the IC fabrication, the study on the dust plasma has drawn a great amount of efforts in recent years.[3−5] The radio frequency (RF) glow discharges between the parallel plates are very suitable for fundamental experimental research on dust plasma. In glow discharges, distinct dust clouds and voids can be observed at the plasma–sheath boundary, near the RF powered electrode.[6,7] Confined in the chamber in various ways, dust particles may nucleate and grow in the discharge,[8−10] which can further be applied for the thin film deposition. Previously, dust particles are commonly obtained by directly feeding dust particles such as pollen, or by etching the target. In our experiment, dust particles were generated in hydrocarbon plasmas;[11−14] the dust particles were generated by two gas-phase reactive materials. It would be more suitable to simulate the microelectronic manufacturing processes, and give basic parameters for improving the quality of discharge. In this study we will compare two cases: discharges of pure Ar and discharges of the mixtures ($SiH_4/C_2H_4/Ar$) containing dust particles. To this end, the curves of the electron density and electron temperature versus the RF power and gas pressure were presented and analysed.

2. Experimental set-up

A simple schematic diagram of the experimental setup is shown in Fig.1, in which a cylindrical reactor powered with capacitively coupled 13.56MHz RF was designed as the discharge chamber. The discharge chamber was mainly composed of three components: a cylindrical glass tube and two stainless steel elec-

*Project supported by the National Natural Science Foundation of China (Grant Nos 10505005 and 10775026).
†E-mail: wangdez@dlut.edu.cn

trodes, the tube serving as a vacuum chamber with dimensions of 120 mm in height and 280 mm in diameter. Inside the chamber, the upper electrode, 300 mm in diameter, was grounded; the RF powered lower circular electrode with a diameter of 50 mm was driven by a matched 13.56 MHz RF voltage source. The separation between these two electrodes was 4 cm. The lower electrode was designed to a special shape to create a trap for the dust particles. In the centre of the inside of the lower electrode, there was a circular hollow hole with 6 mm in depth and 20 mm in diameter. The dust particles would be trapped in the curved sheath above the hollow electrode part.

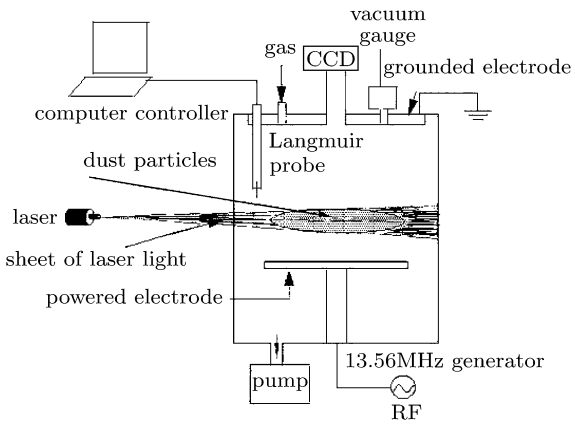


Fig.1. Schematic diagram of the experimental system.

Outside the chamber, an observational window made of fused silica wafer with a diameter of 150 mm, was located in the centre of the upper electrode. Dust particles were illuminated by a thin sheet of He–Ne laser beam. A CCD camera was utilized to record the images from the top and the side. Langmuir probe (Smart Probe^{TM} 0072501(2.3)) with a probe tip of 10 mm in length and 0.19 mm in radius was employed to diagnose the dust plasma at the boundary of dust cloud. The chamber was first pumped by a rotary pump (2XZ-2) to a pressure under 10 Pa, and then pumped by a turbo molecular pump (KYKY FJ-100/110) until the pressure dropped under 10^{-3}Pa. Three mass flow controllers were installed to control the flow rate of reactive gases. The gas pressure could therefore be varied by adjusting the flow rate of a reactive gas during the experiment.

3. Experimental results and discussion

3.1. Observation of dust particles

Invisible particles could grow to visible size (approximately, 2 μm–5 μm) within a minute. They formed a dust cloud, as shown in Fig.2(a), levitating in the RF sheath region. During the process of growth, some particles fled out of the cloud and were lost, while the rest kept staying in the cloud for several hours, and grew to the size of several microns. In the bulk of the plasma, the dust particles kept themselves apart due to the individual particles carrying negative charge. At the same time, the trap confined some of them above the centre of the hollow part on the RF powered electrode.[15]

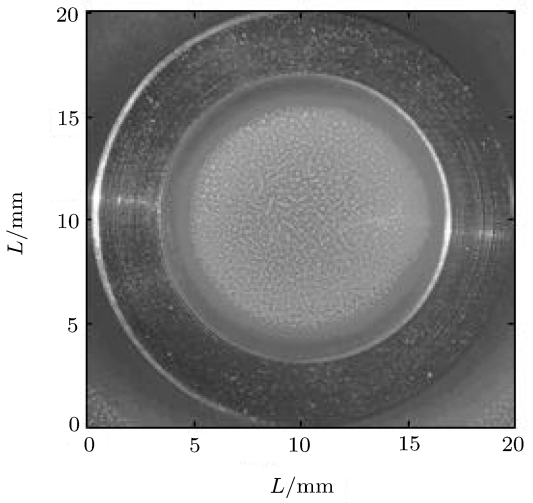


Fig.2. (a) Dust particles trapped in a RF sheath at a pressure of 30 Pa and a power 15W. Under the dust particles is a circular dented electrode part, measuring 20 mm in diameter and 6 mm in depth, which creates a trap for the dust particles.

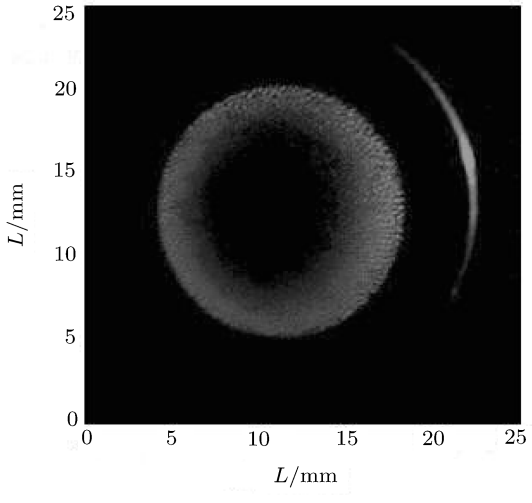


Fig.2. (b) Dust void formed at a RF power of 16 W, and a gas pressure of 63 Pa. The diameter of the dusty void is about 10 mm. A bright, thin circular layer with a diameter of 20 mm and a depth of 6 mm can be seen on the RF powered electrode.

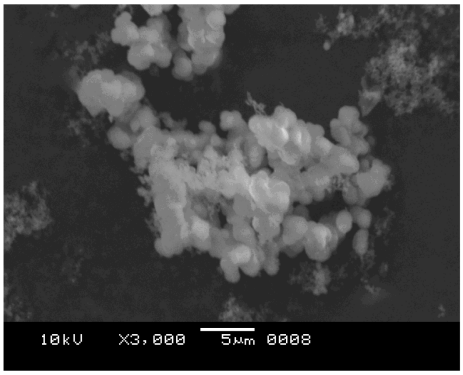


Fig.2. (c) SEM picture of dust particles at a scan voltage 10kV (3000×), with a diameter of 800–1000 nm.

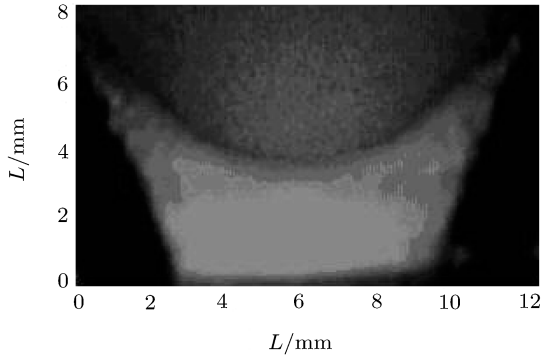


Fig.2. (d) Side view of dust void at a RF power of 15W, and a gas pressure of 48 Pa.

3.2. Diagnosis by Langmuir probe

Langmuir probe was employed to diagnose plasma parameters during observing dust particles. Figure 3 shows the typical $I-V$ characteristic curve. According to the $I-V$ curve and the Laframboise theory,[16,17] the main plasma parameters can be calculated by the Smartsoft program automatically. In this figure, the X axis is the probe bias (V), and the Y axis is the probe current (mA). Scan voltage applied on the probe tip can be varied from –95V to +95V. Since a heavy non-conducting (SiC) contamination layer is built up easily on the probe tip, it has to be removed and cleaned frequently to be kept uncontaminated.

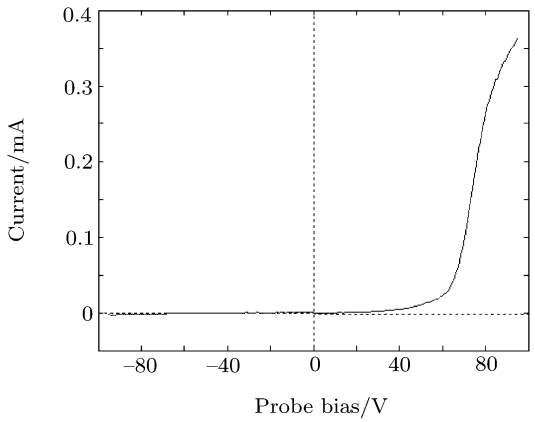


Fig.3. Typical $I-V$ character curve.

Figures 4 and 5 show the variation of the electron density and electron temperature with time in Ar and $SiH_4/C_2H_4/Ar$ discharges respectively. At the beginning of the experiment, only Ar was fed into the chamber, as shown in the region I. The SiH_4 and C_2H_4 were fed into it 100s later. In a very short time, the dust particles formed, as shown in the region II. In the Ar discharge, the gas flow rate was 1.5 sccm, the RF power was 40 W, and the discharge chamber pressure was 23 Pa. In the $SiH_4/C_2H_4/Ar$ discharge, the gas flow rates of SiH_4, C_2H_4, and Ar were all 1.5 sccm, the RF power was 40 W, and the discharge chamber pressure was 42 Pa.

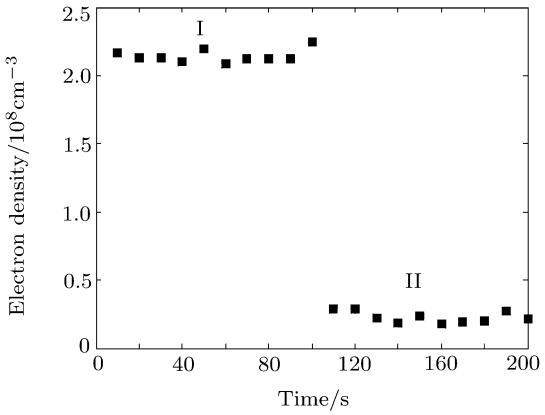


Fig.4. Electron densities in Ar discharge (I) and $SiH_4/C_2H_4/Ar$ discharge (II).

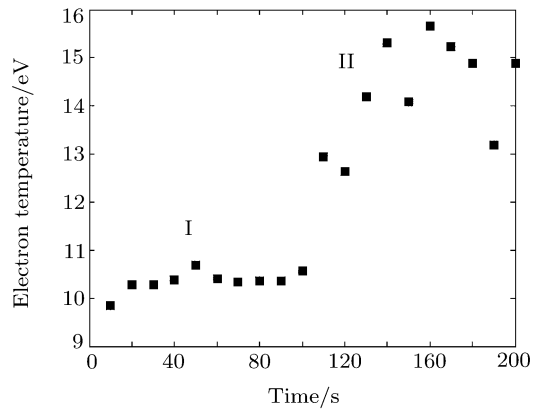


Fig.5. Electron temperatures in Ar discharge (I) and $SiH_4/C_2H_4/Ar$ discharge (II).

From these two figures, it can be seen that in the Ar discharge, the electron temperature is lower than in the $SiH_4/C_2H_4/Ar$ discharge, while the electron density is higher than in the $SiH_4/C_2H_4/Ar$ discharge. In the $SiH_4/C_2H_4/Ar$ discharge, the dust particles with the adsorptive characteristic are produced. Therefore, electrons are adsorbed by the dust particles. That is the reason why most of the dust particles are electronegative. When the electron density drops, the electron temperature rises for maintaining the discharge in the dust plasma as the RF power increases.

3.3. Plasma parameters versus RF power and gas pressure

The curves of electron density and temperature versus the RF power in the boundary of dust cloud are presented in Figs.6 and 7 respectively. The gas flow rates for SiH_4, C_2H_4, and Ar are all set to 1.5 sccm in this experiment. Electron density decreases from 1.6×10^8 to $0.3\times10^8 cm^{-3}$ with the increase of RF power from 20 to 140 W. This curve has a peak value of 2.1×10^8 cm^{-3} at the RF power 50 W. The electron temperature changes from 10 to 21 eV in the region of RF power 10–140 W, and it could reach a maximum value of 21 eV. With the increase of RF power, more electrons would be produced, which have positive effect on the reaction of ethane and silane.

$$SiH_4 + e \rightarrow Si + 2H_2 + e, \quad (1)$$

$$2Si + C_2H_4 \rightarrow 2SiC + 2H_2. \quad (2)$$

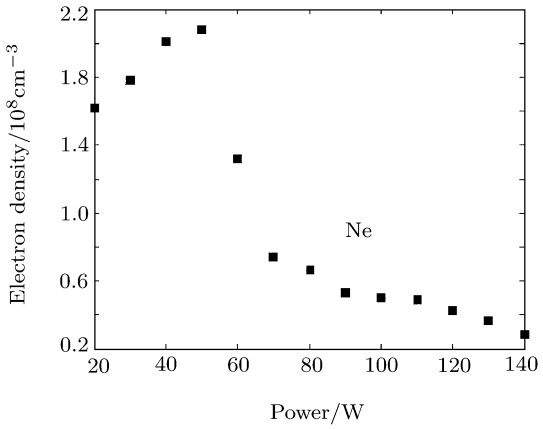


Fig.6. Electron density versus RF power (gas pressure 20Pa).

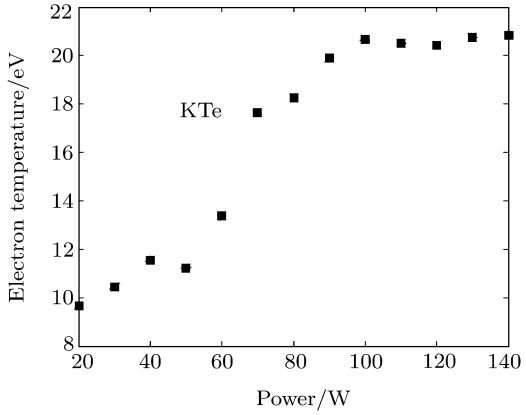


Fig.7. Electron temperature versus RF power (gas pressure 20Pa).

From expressions (1) and (2), it can be concluded that more dust particles (SiC) would form with the increase of the RF power. Due to the increase of dust particles, which have the adsorptive characteristic, many electrons are adsorbed by the dust particles, so the electron density drops. Figure 8 shows that the dust cloud and the void diameters vary with the RF power at a pressure of 63Pa.[18] The size of the dust void versus the RF power first increases and then reduces.

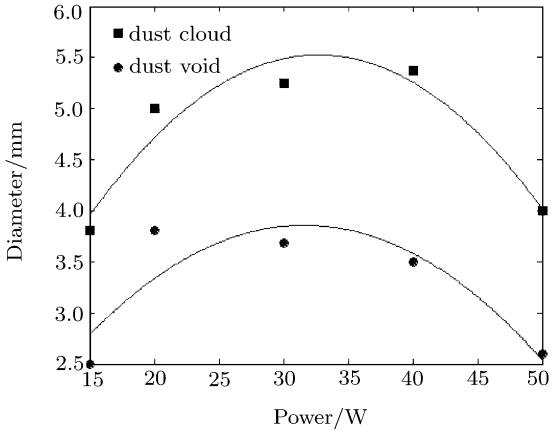


Fig.8. Dust cloud and dust void sizes versus RF power (gas pressure 63Pa).

In the following we present the results in the cases in which the RF power was kept at 20, 60 and 80 W respectively and the pressure of mixtures ($SiH_4/C_2H_4/Ar$) was adjustable. The Ar flow rate was a variable, and C_2H_4 and SiH_4 flow rates were fixed to 1.5 sccm. Consequently, the pressure of the mixtures could be controlled by adjusting the Ar flow rate.

From Fig.9, it can be seen that the electron density increases with the increase of gas pressure. The increase of pressure means that the Ar density rises in the reactive chamber, and accordingly the dust particles are diluted. As a result, the electron density increases due to the decrease of the dust particle density. From Fig.10, it can be seen that the electron temperature drops when the pressure increases. The electron temperature is quite sensitive to the density of dust particles. When the pressure increases, the dust particles produced by SiH_4/C_2H_4 are diluted, and the electron temperature drops. However, the sensitivity of the electron density and the electron temperature to the pressure becomes weaker when the pressure is over 34Pa.

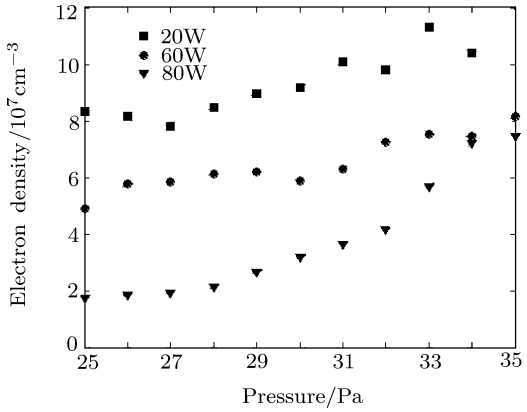


Fig.9. Electron density versus gas pressure for different RF powers.

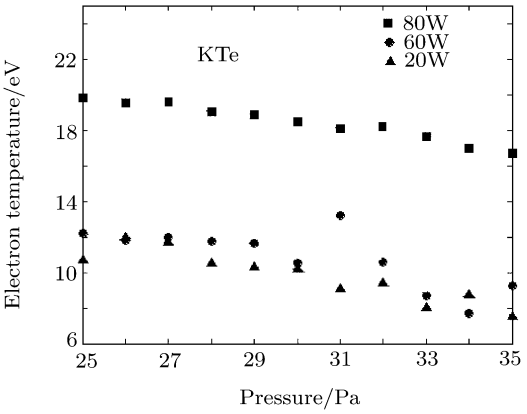


Fig.10. Electron temperature versus gas pressure for different RF powers.

4. Conclusions

In this paper, plasma parameters were measured in a cylindrical discharge chamber powered by a capacitively coupled RF source. It was found that the electron density dropped, and in contrast the electron temperature rose when the dust particles were formed in the $SiH_4/C_2H_4/Ar$ discharges. Because the dust particles of the adsorptive characteristic were generated in the $SiH_4/C_2H_4/Ar$ discharges, a great number of electrons were adsorbed by the dust particles. This explains why most of dust particles are electronegative. When electron density was decreased, the input power rose and the electron temperature also rose for maintaining the discharge.

In addition, the variation of the dust void size with the RF power was also analysed. Although it was not very clear what physical mechanism led to the formation and variation of the dust void in plasma, it was found that the formation of the dust void was sensitive to the dust particle density. The results of the variation of electron density and electron temperature with the RF power showed clearly that the electron temperature first rose, and then gradually reached a steady value. When the RF power increased, more dust particles were generated, and the dust void size then increased. The dust void size would decrease when the chemical reaction reached a balance between silane and ethane. These results might be very useful for understanding the variation of the dust void size with the RF power.

References

[1] Langmuir I, Found G and Dittmer A F 1924 *Science* **60** 392

[2] Roth R M, Spears K G, Stein G D and Wong G 1985 *Appl. Phys. Lett.* **46** 253

[3] He K F and Xie B S 2001 *Chin. Phys.* **10** 214

[4] Xue J K 2006 *Chin. Phys* **15** 562

[5] Huang F, Jiang N, Wang L and Ye M F 2004 *Chin. Phys.* **13** 1896

[6] Selwyn G S,Singh J and Bennett R S 1989 *J. Vac. Sci. Technol.* A **7** 2758

[7] Selwyn G S, Heidenreich J E and Haller K L 1990 *Appl. Phys. Lett.* **57** 1876

[8] Anderson H M, Jairath R and Mock J L 1990 *J. Appl. Phys.* **67** 3999

[9] Liu J W, Xie F Q, Zhong D Y, Wang E G, Liu W X, Li S F and Yang H 2001 *Chin. Phys.* **10** 36

[10] Shiratani M, Fukuzawa T and Watanabe Y 1994 *Plasma Sci.* **22** 103

[11] Deschenaux Ch, Affolter A, Magni D, Hollenstein Ch and Fayet P 1999 *J. Phys.* D *Appl. Phys.* **32** 1876

[12] Stoykov S, Eggs C and Kortshagen U 2001 *J. Phys.* D *Appl. Phys.* **34** 2160

[13] Dolye J R 1997 *J. Appl. Phys.* **82** 4763

[14] Vasile M J and Smolinsky G 1997 *Int. J. Mass Spectrosc. Ion Phys.* **24** 11

[15] Liu D Y, Wang D Z and Liu J Y 2000 *Acta Phys. Sin.* **49** 1094 (in Chinese)

[16] Clements R M 1978 *J. Vac. Sci. Technol.* **15** 193

[17] Hopkins M B and Graham W G 1986 *Rev. Sci. Instrum.* **57** 2210

[18] Wu J, Zhang P Y, Song Q L, Zhang J L and Wang D Z 2005 *Acta Phys. Sin.* **54** 4794 (in Chinese)